Lasers in Surgery and Medicine 9999:1–5 (2016)

Investigating Skin Penetration Depth and Shape Following Needle-Free Injection at Different Pressures: A Cadaveric Study

Joon Seok, MD,[1] **Chang Taek Oh**, MS,[2] **Hyun Jung**[Q1] **Kwon**, MD,[1] **Tae Rin Kwon**, PhD,[2] **Eun Ja Choi**, BS,[2] **Sun Young Choi**, MD,[1] **Seok Kyun Mun**, MD, PhD,[3] **Seung Ho Han**, MD, PhD,[4] **Beom Joon Kim**, MD, PhD,[1]* and **Myeung Nam Kim**, MD, PhD[1]

[1]*Department of Dermatology, Chung-Ang University College of Medicine, Seoul, Korea*
[2]*Department of Medicine, Graduate School, Chung-Ang University, Seoul, South Korea*
[3]*Department of Otorhinolaryngology-Head and Neck Surgery, Chung-Ang University College of Medicine, Seoul, Korea*
[4]*Department of Anatomy, Chung-Ang University College of Medicine, Seoul, Korea*

Background and Objectives: The effectiveness of needle-free injection devices in neocollagenesis for treating extended skin planes is an area of active research. It is anticipated that needle-free injection systems will not only be used to inject vaccines or insulin, but will also greatly aid skin rejuvenation when used to inject aesthetic materials such as hyaluronic acid, botulinum toxin, and placental extracts. There has not been any specific research to date examining how materials penetrate the skin when a needle-free injection device is used. In this study, we investigated how material infiltrates the skin when it is injected into a cadaver using a needle-free device.

Study Design/Materials and Methods: Using a needle-free injector (INNOJECTOR™; Amore Pacific, Seoul, Korea), 0.2 ml of 5% methylene blue (MB) or latex was injected into cheeks of human cadavers. The device has a nozzle diameter of 100 μm and produces a jet with velocity of 180 m/s. This jet penetrates the skin and delivers medicine intradermally via liquid propelled by compressed gasses. Materials were injected at pressures of 6 or 8.5 bars, and the injection areas were excised after the procedure. The excised areas were observed visually and with a phototrichogram to investigate the size, infiltration depth, and shape of the hole created on the skin. A small part of the area that was excised was magnified and stained with H&E (×40) for histological examination.

Results: We characterized the shape, size, and depth of skin infiltration following injection of 5% MB or latex into cadaver cheeks using a needle-free injection device at various pressure settings. Under visual inspection, the injection at 6 bars created semi-circle-shaped hole that penetrated half the depth of the excised tissue, while injection at 8.5 bars created a cylinder-shaped hole that spanned the entire depth of the excised tissue. More specific measurements were collected using phototrichogram imaging. The shape of the injection entry point was consistently spherical regardless of the amount of pressure used. When injecting 5% MB at 6 bars, the depth of infiltration reached 2.323 mm, while that at 8.5 bars reached 8.906 mm. The area of the hole created by the 5% MB injection was 0.797 mm^2 at 6 bars and 0.242 mm^2 at 8.5 bars. Latex injections reached a depth of 3.480 mm at 6 bars and 7.558 mm at 8.5 bars, and the areas were measured at 1.043 mm^2 (6 bars) and 0.355 mm^2 (8.5 bars). Histological examination showed that the injection penetrated as deep as the superficial musculoaponeurotic system at 6 bars and the masseter muscle at 8.5 bars.

Conclusion: When injecting material into the skin using a pneumatic needle-free injector, higher-pressure injections result in a hole with smaller area than lower-pressure injections. The depth and shape of skin penetration vary according to the amount of pressure applied. For materials of low density and viscosity, there is a greater difference in penetration depth according to the degree of pressure. Lasers Surg. Med. 9999:1–5, 2016.

Key words: cadaver; depth; needle-free injector; needle-less microjet device; penetration; pressure; shape

INTRODUCTION

Needle-free injection devices have previously been used to inject macromolecules such as insulin and vaccines into the skin. Recent studies on these devices have shown their effect on scar remodeling through stimulation of fibroblasts by

Conflict of Interest Disclosures: All authors have completed and submitted the ICMJE Form for Disclosure of Potential Conflicts of Interest and none were reported.

Joon Seok and Chang Taek Oh should be considered as co-first authors.

Contract grant sponsor: Ministry of Health & Welfare, Republic of Korea.

*Correspondence to: Beom Joon Kim, MD, PhD, Department of Dermatology, Chung-Ang University Hospital 224-1 Heukseok-dong, Dongjak-ku, Seoul 156-755, South Korea, E-mail: beomjoon@unitel.co.kr

Accepted 20 March 2016
Published online in Wiley Online Library (wileyonlinelibrary.com).
DOI 10.1002/lsm.22517

micro-trauma and activation of neocollagenesis, as well as their capacity to treat extended skin planes [1,2]. Needle-free injection device treatment is also effective for wrinkle reduction without any side effects [2]. Furthermore, these devices can be used to treat depressed scars due to herpes zoster, acne, and tissue necrosis following filler injection [3–5]. On a hypertrophic scar of the forehead, treatment using a needle-free injector device caused a protruding scar to become flat [6]. Needle-free injection systems will likely be used to inject various aesthetic materials such as hyaluronic acid (HA), botolinum toxin, and placental extracts into the skin to aid skin rejuvenation [7]. Needle-free injection devices also reduce the amount of pain experienced by patients, result in only minimal skin response, and prevent certain hazards caused by more conventional treatment methods such as skin puncture and destruction [8]. However, there has not been any specific research into how materials penetrate the skin when using a needle-free injection device. In this study, we investigated how materials infiltrate tissue when injected into a cadaver using a needle-free injection device.

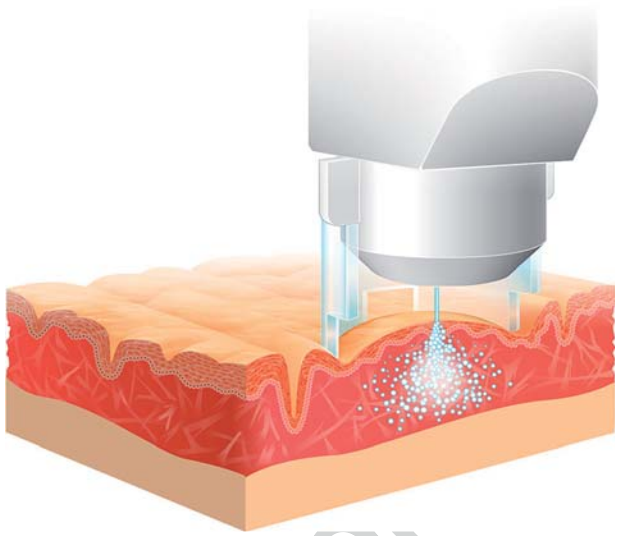

Fig. 1. The mechanism of the needle-free injection device.

MATERIALS AND METHODS

Injections were performed using six human cadavers prior to being embalmed. Either 0.2 ml of 5% MB (density: 1.01 g/ml, DA-645, KEM, Tokyo, Japan) (viscosity: 13.1 centipoise, 13.1 g/m · s, LVDV-II + Pro, Brookfield Engineering Laboratories, Inc., MA) or cadaver injection latex (EG-LT-1010, E.G.O Lab, Seoul, Korea) (density: 1.10 g/ml, viscosity: 557.1 centipoise, 557.1 g/m · s, LVDV-II + Pro, Brookfield Engineering Laboratories, Inc., MA) was injected into the cheek areas of cadavers using a needle-free injector (INNOJECTOR™; Amore Pacific, Seoul, Korea) (Fig. 1). This device has a nozzle diameter of 100 μm that generates a high-velocity jet (180 m/s) to permeate the skin and transfer medicine intradermally via liquid propelled by compressed gas.

Injections were performed at pressures of 6 and 8.5 bars (Fig. 2a). Tissue was excised after injection (Fig. 2b), and the size, depth of infiltration, and shape of the hole caused by injection were investigated through visual inspection. A phototrichogram (×15) (Folliscope 4.0, Lead M, Seoul, Korea) and H&E (×40) staining were also performed to allow for more precise measurements of the area.

All statistical analyses were performed using SPSS for Windows (v19; IBM SPSS, Armonk, NY). The χ^2 test and independent *t*-test were used to compare continuous variables. Data with $P < 0.05$ were considered statistically significant. We interpreted *P*-values less than 0.001 as highly significant.

RESULTS

We characterized the shape, size, and depth of skin infiltration following injection of 5% MB or latex into cadaver cheeks using a needle-free injection device at various pressure settings. Latex, a material with a higher viscosity than aesthetic medicines such as hyaluronic acid (HA) and placental extract, was injected to assess the degree to which aesthetic medicines would infiltrate skin. Under visual inspection, the depth of infiltration following injection of either 5% MB or latex differed according to the injection pressure (Fig. 3). At 8.5 bars, the materials penetrated the full thickness of the excised tissue in a cylindrical shape, while at 6 bars, the materials penetrated half of the thickness of the excised tissue in the shape of a semi-circle (Fig. 3). These results were confirmed with a phototrichogram, which additionally demonstrated that the hole generated by injection was spherical regardless of the degree of pressure or material used (Fig. 4). At 8.5 bars, penetration reached the bottom of the excision area in a cylinder shape, as with the previous MB injection (Fig. 4a). The penetration reached as far as the middle point of the excision area, in the shape of a horizontally spread upper hemisphere (Fig. 4b).

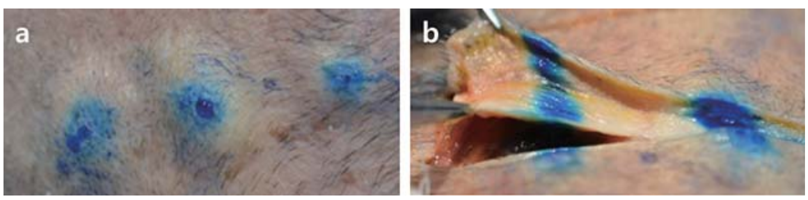

Fig. 2. (**a**) 5% MB injection with a[Q2] needle-free injector. (**b**) Excision of cadaveric skin to investigate the penetration depth and shape resulting from injection.

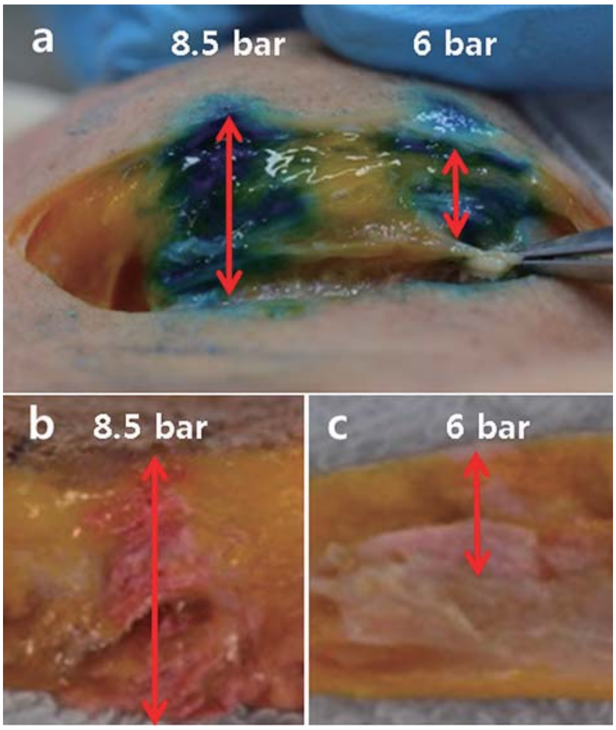

Fig. 3. Gross morphologic forms after excision. (**a**) 5% MB injection at pressure levels of 6 and 8.5 bars. (**b**) Latex injection at pressure levels of 6 and 8.5 bars. (**c**) Latex injection at pressure levels of 6 bars.

The area of the hole created following needle-free injection of 5% MB was significantly greater at 6 bars (0.797 mm^2, Standard deviation, Std: 0.366) than at 8.5 bars (0.242 mm^2, Std: 0.418) ($P < 0.001$). A similar result was found following latex injection, where the area of the hole generated at 6 bars was 1.043 mm^2 (Std: 0.468), while that at 8.5 bars was 0.355 mm^2 (Std: 0.119) ($P = 0.010$) (Fig. 5). On the other hand, there was no significant difference in hole size created by 5% MB and latex at either 6 bars ($P = 0.305$) or 8.5 bars ($P = 0.412$).

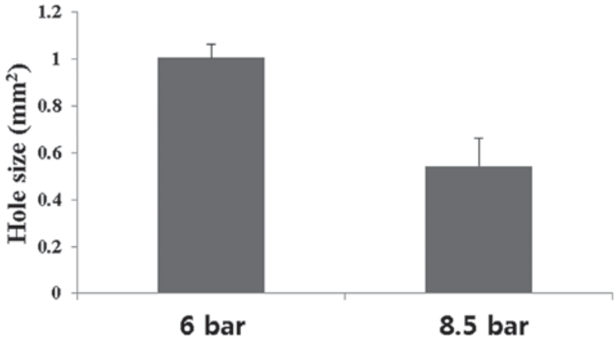

Fig. 5. Total area of the hole caused in the skin due to pressure after skin injection (mm^2). When injecting 5% MB, the area of the hole created at the injection was 3.186 mm^2 at 6 bars and 0.967 mm^2 at 8.5 bars. When latex was injected, the area of the hole generated 4.172 mm^2 at 6 bars and 0.355 mm^2 at 8.5 bars. ($^{*}P < 0.05$, $^{***}P < 0.001$).

When injecting 5% MB, the depth of penetration was 2.330 mm (Std: 0.273) at 6 bars and 8.906 mm (Std: 0.289) at 8.5 bars ($P < 0.001$). When latex was injected, the depth of penetration reached 3.480 mm (Std: 0.482) at 6 bars and 7.558 mm (Std: 0.263) at 8.5 bar ($P < 0.001$). Of note, there was also a significant difference in depth of penetration when injecting 5% MB or latex at both pressure settings ($P < 0.001$) (Fig. 6).

Histological observation showed that, at 6 bars, penetration reached beyond the subcutaneous tissue and into the superficial musculoaponeurotic system (SMAS) (Fig. 7a). At 8.5 bar, penetration passed beyond the SMAS into the masseter muscle (Fig. 7b).

DISCUSSION

Shergold et al. reported that liquid jets of high velocity penetrate human skin by forming and opening cracks [9]. In our study, we demonstrate that higher injection pressures result in smaller total area of tissue penetration. Our study also confirmed that the depth and shape of skin

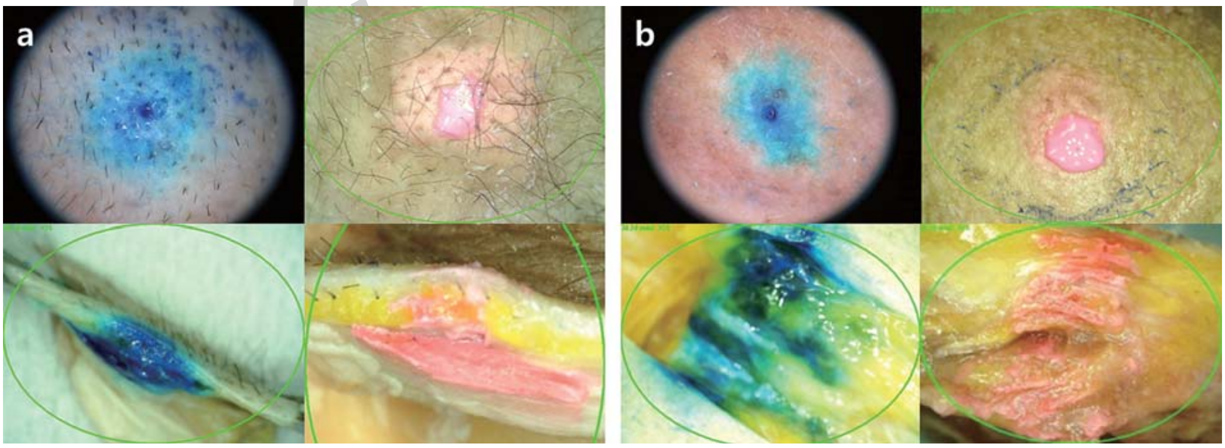

Fig. 4. Phototrichogram photographs magnified 15 times. (**a**) 6 bars with 5% MB (left panel) and latex (right panel). (**b**) 8.5 bars with 5% MB (left panel) and latex (right panel).

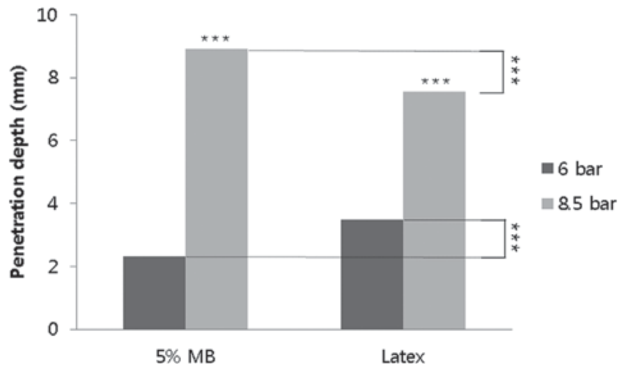

Fig. 6. Depth of penetration materials in cadaveric skin injected from a needle-free injector (mm). When injecting 5% MB, the depth of penetration was 2.330 mm at 6 bars and 8.906 mm at 8.5 bars. When latex was injected, the depth of penetration reached 3.480 mm at 6 bars and 7.558 mm at 8.5 bars. ($^{*}P < 0.05$, $^{***}P < 0.001$).

penetration differed according to the amount of pressure. At the same pressure, there was no significant difference in the areas of holes created by different density and viscosity materials. However, there was a trend that higher density and viscosity material produced larger area holes than did lower density/viscosity materials. On the other hand, there was a significant difference in penetration depth of materials with different viscosity and density when injected at the same pressure.

The current understanding is that, when jet dispersion occurs on skin, it occurs in a fan-like pattern resembling an expanding jet [10]. When dispersion occurs, the flow begins to spread from a single point, creating a circular pattern. The point of dispersion reaches a greater depth as the jet velocity and nozzle diameter increase, acting as a marker of penetration depth and shape [11]. Schramm-Baxter et al. showed that, at 160 m/s with a nozzle diameter of 31 μm, the depth of penetration reached the epidermis and superficial dermis. In addition, the depth of penetration went beyond the dermis floor when the nozzle diameter was 229 μm. This study also found that the shape of dispersion varied according to nozzle size, with resulting semi-circular holes at 76 μm, an ellipsoid at 152 μm, and semi-circular holes at 229 μm [12]. When velocity was reduced to 110 m/s with a nozzle diameter of 152 μm, dispersion occurred in the form of a semi-circle. When velocity was increased to 190 m/s, a semi-circular-shaped dispersion occurred with maximal spread near the bottom [12]. In addition to nozzle diameter and velocity, the amount of pressure applied has a significant effect on the depth and shape of penetration. Our results show that the dispersion formed the shape of a semi-circle at a pressure of 6 bars and the form of a cylinder at a pressure of 8.5 bars.

Previous research suggests that, after injection, the injected material spreads from a single point on the skin to form a spherical shape. If the provided propulsion is not sufficient to infiltrate the layer below, stagnation pressure pushes the material into a wide spherical pattern. If penetration occurs through all layers of the skin due to great force, then the injection is expected to form a cylinder-shaped pattern as no stagnation occurs. Velocity also plays a very important role in the completeness of jet penetration. At 60–80 m/s, material cannot infiltrate the skin. Above this threshold, the degree to which penetration occurs monotonically increases at a velocity of approximately 150 m/s, and near 100% delivery is achieved [13]. A velocity of 180 m/s was used in this study, ensuring that all material was delivered into the skin.

When using a needle-free jet injector, a large particle size resulted in less dispersion and penetration below the dermis. This is due to jet energy dissolving through friction with the skin [14]. With large particles, accumulation in the skin continues with lower release rates [14]. Depending on the particle size of the substance being injected, depth of penetration into the skin and duration of treatment effect will differ.

Skin parameters such as Young's modulus, a measure of cutaneous rigidity, affect the skin penetration depth [13,15]. At constant jet velocity and nozzle diameter, the depth of penetration decreases with increasing Young's modulus [13]. Escoffier et al. reported that skin extensibility remains constant until approximately 70 years of age, at which time it begins to decline [16]. They also demonstrated a 20% increase in Young's modulus after reaching 70 years of age [16]. With this in mind, higher

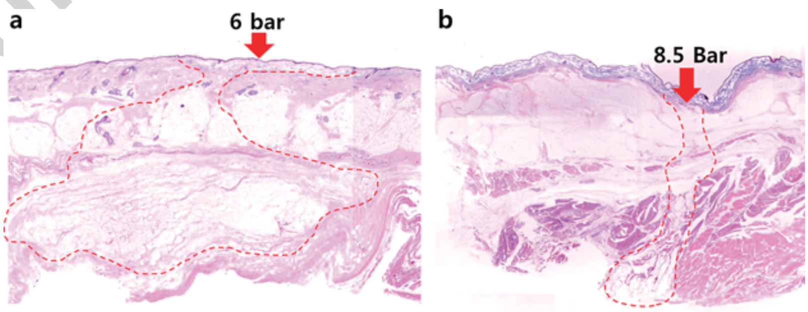

Fig. 7. Histological analysis (H&E, ×40). (**a**) Upper hemisphere shape penetration to SMAS at pressure level of 6 bars. (**b**) Cylindrical shape penetration to masseter muscle at pressure level of 8.5 bars.

pressures should be applied for jet injections in patients 70 years of age or older compared with a younger patient in order to reach the same level of penetration. Conversely, aging results in reduced skin thickness, decreased collagen and elastin, and impaired skin cell organization, leading to possible damage to the skin barrier with high-pressure injection [16–19].

Fresh human cadavers are the most viable alternative option to live human experiments. Cadavers are commonly utilized during surgical education [20]. Depending on the duration of time after death, cadaveric tissue begins to lose some characteristics of live tissue such as elasticity and consistency [21]. As such, our study does have some limitations. Although fresh cadavers were used, injections were not made into living skin. For this reason, Young's modulus is different from that of living human skin, though the exact difference could not be measured. Joy et al. demonstrated a 15.0 kPa Young's modulus of masseter muscle in cadavers, which is lower than reported measurements in live human tissue (31.0 kPa) [22,23]. We expect that the higher Young's modulus in live tissue would result in weaker penetration of injected materials. It is also likely that it would be necessary to apply slightly higher pressures than those used in this study to reach the same depth of penetration in living skin.

In the future, additional studies must be performed to determine whether macromolecule materials that are used as injection materials, such as hyaluronic acid filler, botox, and placenta extract, maintain their characteristics and stability when they are injected with high pressure and velocity.

CONCLUSIONS

This study showed that during injection of material into skin with a pneumatic needle-free injector, the amount of pressure applied changes the size of the hole created by the injection, skin penetration depth, and shape. Using these findings, we can selectively choose injection materials to achieve the appropriate depth and scope.

ACKNOWLEDGMENTS

This study was supported by "User (Hospital) Test for Domestic New Medical Device" of the Korea Health Industry Development Institute (KHIDI), funded by the Ministry of Health & Welfare, Republic of Korea.

REFERENCES

1. Stachowiak JC, Li TH, Arora A, Mitragotri S, Fletcher DA. Dynamic control of needle-free jet injection. J Control Release 2009;135:104–112.
2. Levenberg A, Halachmi S, Arad-Cohen A, Ad-El D, Cassuto D, Lapidoth M. Clinical results of skin remodeling using a novel pneumatic technology. Int J Dermatol 2010;49:1432–1439.
3. Kim BJ, Yoo KH, Kim MN. Successful treatment of depressed scars of the forehead secondary to herpes zoster using subdermal minimal surgery technology. Dermatol Surg 2009;35:1439–1440.
4. Lee JW, Kim BJ, Kim MN, Lee CK. Treatment of acne scars using subdermal minimal surgery technology. Dermatol Surg 2010;36:1281–1287.
5. Seok J, Choi SY, Park KY, Jang JH, Bae JH, Kim BJ, Kim MN, Hong CK. Depressed scar after filler injection successfully treated with pneumatic needleless injector and radiofrequency device. Dermatol Ther (epub) 2015.
6. Seok J, Hong JY, Jang JH, Bae JH, Choi SY, Yoo KH, Kim BJ. The NEEDLELESS[Q3] MICROJET: A novel device for hypertrophic scar remodelling on the forehead. J Eur Acad Dermatol Venereol (epub) 2015.
7. Kobus KF, Dydymski T. Quantitative dermal measurements following treatment with AirGent. Aesthet Surg J 2010;30: 725–729.
8. Patwekar SL, Gattani SG, Pande MM. Needle free injection system: A review. Int J Pharm Pharm Sci 2013;5:14–19.
9. Shergold OA, Fleck NA, King TS. The penetration of a soft solid by a liquid jet, with application to the administration of a needle-free injection. J Biomech 2006;39:2593–2602.
10. Seyam RM, Bégin LR, Tu LM, Dion SB, Merlin SL, Brock GB. Evaluation of a no-needle penile injector: A preliminary study evaluating tissue penetration and its hemodynamic consequences in the rat. Urology 1997;50:994–998.
11. Chen K, Zhou H, Li J, Cheng GJ. A model on liquid penetration into soft material with application to needle-free jet injection. J Biomech Eng 2010;132:101005.
12. Schramm-Baxter J, Mitragotri S. Needle-free jet injections: Dependence of jet penetration and dispersion in the skin on jet power. J Control Release 2004;97:527–535.
13. Baxter J, Mitragotri S. Jet-induced skin puncture and its impact on needle-free jet injections: Experimental studies and a predictive model. J Control Release 2005;106:361–373.
14. Michinaka Y, Mitragotri S. Delivery of polymeric particles into skin using needle-free liquid jet injectors. J Control Release 2011;153:249–254.
15. Agache PG, Monneur C, Leveque JL, De Rigal J. Mechanical properties and Young's modulus of human skin in vivo. Arch Dermatol Res 1980;269:221–232.
16. Escoffier C, de Rigal J, Rochefort A, Vasselet R, Lévêque JL, Agache PG. Age-related mechanical properties of human skin: An in vivo study. J Invest Dermatol 1989;93: 353–357.
17. Callaghan TM, Wilhelm KP. A review of ageing and an examination of clinical methods in the assessment of ageing skin. Part I: Cellular and molecular perspectives of skin ageing. Int J Cosmet Sci 2008;30:313–322.
18. Kim E, Cho G, Won NG, Cho J. Age-related changes in skin bio-mechanical properties: The neck skin compared with the cheek and forearm skin in Korean females. Skin Res Technol 2013;19:236–241.
19. Luebberding S, Krueger N, Kerscher M. Mechanical properties of human skin in vivo: A comparative evaluation in 300 men and women. Skin Res Technol 2014;20: 127–135.
20. Gerad JM, Ohayon J, Luboz V, Perrier P, Payan Y. Nonlinear elastic properties of the lingual and facial tissues assessed by indentation technique application to the biomechanics of speech production. Med Eng Phys 2005;27:884–892.
21. Lim YJ, Deo D, Singh TP, Jones DB, De S. In situ measurement and modeling of biomechanical response of human cadaveric soft tissues for physics-based surgical simulation. Surg Endosc 2009;23:1298–1307.
22. Joy J, McLeod G, Lee N, Munirama S, Corner G, Eisma R, Cochran S. Quantitative assessment of thiel soft-embalmed human cadavers using shear wave elastography. Ann Anat 2015;202:52–56.
23. Luboz V, Promayon E, Payan Y. Linear elastic properties of the facial soft tissues using an aspiration device: Towards patient specific characterization. Ann Biomed Eng 2014;42: 2369–2378.